The Astrophysical Journal, 623:383–391, 2005 April 10

HIGH- AND LOW-FREQUENCY QUASI-PERIODIC OSCILLATIONS IN THE X-RAY LIGHT CURVES OF THE BLACK HOLE TRANSIENT H1743−322

Jeroen Homan,[1] Jon M. Miller,[2,3] Rudy Wijnands,[4] Michiel van der Klis,[4] Tomaso Belloni,[5] Danny Steeghs,[2] and Walter H. G. Lewin[1]

Received 2004 June 14; accepted 2004 August 5

ABSTRACT

We present a variability study of the black hole candidate and X-ray transient H1743−322 during its 2003–2004 outburst. We analyzed five *Rossi X-Ray Timing Explorer* observations that were performed as part of a multiwavelength campaign, as well as six observations from the early rise of the outburst. The source was observed in several black hole states and showed various types of X-ray variability, including high-frequency quasi-periodic oscillations (QPOs) at 240 and 160 Hz (i.e., with a 3:2 frequency ratio), several types of low-frequency QPOs, and strong variations on a timescale of a few hundred seconds. The discovery of high-frequency QPOs in H1743−322 supports predictions that these QPOs should be more easily observed in high inclination systems. In one of our observations a transition in count rate and color occurred, during which we were able to follow the smooth evolution of the low-frequency QPOs from type B to type A. We classify the X-ray observations and QPOs and briefly discuss the QPOs in terms of recently proposed models.

Subject headings: stars: individual (H1743−322) — stars: oscillations — X-rays: binaries — X-rays: stars

1. INTRODUCTION

Outbursts of transient X-ray binaries provide excellent opportunities to study the properties of accretion flows onto compact objects over a large range of mass accretion rates. Black hole transients are in general more luminous and show more pronounced changes in their spectral and variability properties than neutron star transients. Past observations of black hole transients have revealed an intriguing variety of correlated spectral and variability properties that is often described in terms of so-called black hole states and transitions between them (Tanaka & Lewin 1995; van der Klis 1995a; McClintock & Remillard 2004). Three such states are generally recognized: the hard state, the soft (or thermal-dominant) state, and the very high (or steep power law) state (see McClintock & Remillard 2004 for a recent discussion). It has been found that not only the X-ray properties change from one state to the other, but that major changes in the radio (e.g., Fender et al. 1999), optical (e.g., Jain et al. 2001), and IR (e.g., Homan et al. 2004) occur as well. As these different wavelengths probe different regions and mechanisms in the accretion flow, it is important to obtain simultaneous data in order to construct a consistent picture of the accretion flow. To this end we organized a multiwavelength campaign—using *RXTE*, *Chandra*, radio, and optical observations—to study a black hole transient in outburst. This program was triggered by an outburst of H1743−322 in 2003 March. Results of the analysis of the X-ray spectra are reported by Miller et al. (2004). The results of radio observations made in partial support of this program will be reported in a separate paper by M. P. Rupen et al. (2004, in preparation), and results from optical and IR observations will be reported in D. Steeghs et al. (2004, in preparation). Here we report on the variability properties of the *RXTE* observations, focusing on the quasi-periodic oscillations (QPOs).

Different types of black hole QPOs were already found with *Ginga* in several sources (e.g., Miyamoto et al. 1991; Takizawa et al. 1997), but it was not until a few years ago that they were classified in a systematic way. Wijnands et al. (1999) and Remillard et al. (2002c) recognized three types of low-frequency (<10 Hz) QPOs in XTE J1550−564, which they named types A, B, and C. The strongest of these, type C, have frequencies ranging from tens of mHz to ∼10 Hz. They are always accompanied by strong band-limited noise (i.e., with a clear break in the power as function of frequency) and are associated with the hard state and transitions to and from the soft state. Type A and B QPOs, found only in the very high/steep power law state, are confined to a narrow frequency range of ∼4–9 Hz and are accompanied by weak power law noise (red noise). Type B QPOs are more coherent and have a higher harmonic content. All three QPO types also have unique time lag properties (Wijnands et al. 1999; Remillard et al. 2002c), showing both hard and soft lags, that are hard to explain with simple Comptonization models. Unfortunately, the large variety of black hole QPOs is not well understood. Almost every black hole X-ray transient has shown one or more of these three QPO types, although not all observed QPOs can be classified within this scheme (see, e.g., Remillard et al. 2002c). For example, a weak QPO around 20 Hz has been observed during the soft states of XTE J1550−564 (Homan et al. 2001) and GRO J1655−40 (Sobczak et al. 2000). Other types of low-frequency QPOs were found in 4U 1630−47 (∼0.1 Hz; Dieters et al. 2000) and GRS 1915+105 (∼0.01 Hz; Morgan et al. 1997). These QPOs were often present simultaneously with type A, B, or C QPOs and possibly represent fast transitions between different (sub)states (see, e.g., the dynamical power spectra in Muno et al. 1999). High-frequency (>50 Hz) QPOs have also been found in a small number of systems. They appear to be stable in frequency, and in a few cases two harmonically related

[1] MIT Center for Space Research, 70 Vassar Street, Cambridge, MA 02139.
[2] Harvard-Smithsonian Center for Astrophysics, 60 Garden Street, Cambridge, MA 02138.
[3] NSF Astronomy and Astrophysics Fellow.
[4] Astronomical Institute "Anton Pannekoek," University of Amsterdam, Kruislaan 403, 1098 SJ Amsterdam, Netherlands.
[5] INAF/Osservatorio Astronomico di Brera, Via E. Bianchi 46, I-23807 Merate (LC), Italy.

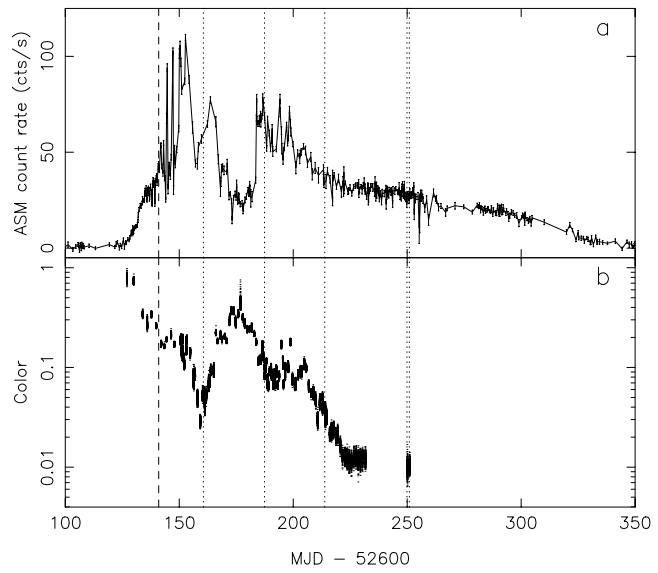

FIG. 1.—Light and color curves of the 2003–2004 outburst of H1743−322. (*a*) *RXTE* ASM light curve (∼2–12 keV). (*b*) Color curve, obtained from *RXTE* PCA data (higher values indicating a harder spectrum). The five dotted lines mark the times of our (quasi-)simultaneous *RXTE*/*Chandra* observations. Observations a–f were all made before the dashed line.

peaks (with frequency ratios of 3:2 or 5:3) have been observed at the same time (Strohmayer 2001a, 2001b; Miller et al. 2001), which have been used to constrain the spin of the black hole.

H1743−322 was discovered in 1977 August with *Ariel 5* (Kaluzienski & Holt 1977a, 1977b) as a new transient "with a spectrum somewhat harder than the Crab" (Doxsey et al. 1977; *HEAO 1* observations). The outburst lasted until at least 1978 March (Wood et al. 1978). White & Marshall (1983) identified the source as a potential black hole candidate based on its ultrasoft X-ray spectrum, which was similar to that of other black hole candidates in their soft state. High-energy observations during the 1977–1978 outburst also revealed the presence of a high-energy tail in the spectrum (Cooke et al. 1984). A new outburst of the source was detected[6] with *INTEGRAL* (Revnivtsev et al. 2003) and *RXTE* (Markwardt & Swank 2003a, 2003b) in 2003 March that lasted until early 2004 (see Fig. 1). The only reported detections of the source between the 1977–1978 and 2003–2004 outbursts were with *EXOSAT* in 1984 (Reynolds et al. 1999) and the TTM/COMIS telescope (2–30 keV) on board *Mir-Kvant* in 1996 (Emelyanov et al. 2000). Soon after the *INTEGRAL* and *RXTE* detections, radio (Rupen et al. 2003), infrared (Baba et al. 2003), and optical (Steeghs et al. 2003) counterparts were found. *INTEGRAL* and *RXTE* observations suggest that the source went through several states during its outburst (Markwardt & Swank 2003a; Homan et al. 2003b; Kretschmar et al. 2003; Grebenev et al. 2003; Tomsick & Kalemci 2003; Parmar et al. 2003; Kalemci et al. 2004). Markwardt & Swank (2003a) found a 0.05 Hz QPO with an rms amplitude of 25% during the early stages of the outburst, typical of the hard state. Homan et al. (2003b) already reported on QPOs around 6 Hz (see also Spruit et al. 2004) and the discovery of a QPO at 240 Hz. QPOs around 8 Hz were found by Tomsick & Kalemci (2003) when the source was making a transition back to the hard state. In this paper we present a more detailed study of the high-frequency QPO and the evolution of the lower frequency QPOs during a rapid transition in the light curve.

[6] The new detection led to the addition of the following source identifiers: IGR J17464−3213 and XTE J1746(4)−322. In the literature the source is sometimes also referred to as H1741−32. In the *RXTE* archive the source can be found as XTE J1746−319.

2. OBSERVATIONS AND DATA ANALYSIS

We observed H1743−322 with *RXTE* (Bradt et al. 1993) on five occasions between 2003 May 1 and July 31. These observations, which were all part of program P80135, spanned multiple *RXTE* observation IDs, and most of these contained multiple *RXTE* orbits. A log of the observations can be found in Table 1. Observations 1–3 and 5 were performed simultaneously with *Chandra* observations. Spectral results from these combined observations are reported by Miller et al. (2004). The variability study in this paper is solely based on data from the proportional counter array (PCA, consisting of five similar units; Jahoda et al. 1996) on board *RXTE*. The PCA data we used were in the following modes: Standard 2, which has a time resolution of 16 s and covers the 2–60 keV PCA effective energy range with 129 energy channels; SB_125us_8_13_1s and SB_125us_14_35_1s, which have a time resolution of 2^{-13} s (∼122 μs) and cover the 3.3–5.8 and 5.8–14.9 keV bands with one channel; and finally, E_16us_16B_36_1s, which has a time resolution of 2^{-16} s (∼15 μs) and covers the 14.9–60 keV band with 16 channels. Standard 2 data from proportional counter unit (PCU) 2 were background-subtracted and then used to create light curves and color curves, with color defined as the ratio of counts in the 9.5–17.9 and 2.5–5.8 keV bands (Standard 2 channels 20–40 and 3–10).

TABLE 1
LOG OF OUR FIVE *RXTE* PCA OBSERVATIONS OF H1743−322

Observation	Date	Start–Stop[a] (UTC)	Total (ks)	Counts s^{-1}	rms[b] (%)
1	2003 May 1	17 00–02 03	24.3	1760.0 ± 0.2	10.19 ± 0.10
2	2003 May 28	05 29–16 53	24.6	2037.4 ± 0.3	10.87 ± 0.09
	...	Before	4.9	1824.1 ± 0.6	10.02 ± 0.15
	...	After	19.7	2091.2 ± 0.3	11.11 ± 0.09
3	2003 Jun 23	17 05–22 43	13.7	1120.4 ± 0.3	5.4 ± 0.3
4	2003 Jul 29	20 54–22 51	4.7	752.1 ± 0.6	5.3 ± 0.8[c]
5	2003 Jul 30	19 49–00 43	2.4	757.1 ± 0.7	5.3 ± 0.8[c]

[a] Observations 1 and 5 ended the next day. "Before" and "after" for observation 2 refer to before and after the transition in the light curve.
[b] Fractional rms amplitude (5.8–20.9 keV) in the 0.016–100 Hz range.
[c] Measured from the combined power spectra of observations 4 and 5.

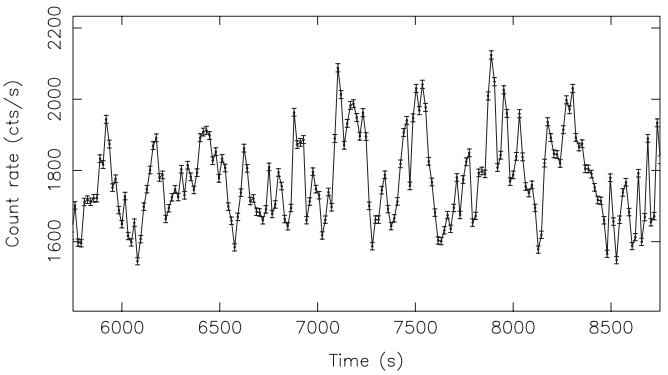

FIG. 2.—Example of strong variability on a timescale of a few hundred seconds, as observed in observations 1–3. This light curve (2–60 keV) is from observation 1. It is background-subtracted and has a time resolution of 32 s.

Fast Fourier transforms (FFTs) of the high time resolution data from all the active PCUs[7] were performed to create power spectra with a frequency range of 0.016–4096 Hz in the 5.8–20.9 keV band (absolute channels 14–49). This energy range was chosen since high-frequency variability in black hole low-mass X-ray binaries is in general most significantly detected in similar energy ranges. The data were not background-subtracted, and no dead-time corrections were applied prior to the FFTs; the effects of dead time were accounted for by our power spectral fit function (see below). Power spectra were averaged based on time, colors, or count rate and normalized according to the recipe described in van der Klis (1995b).

As in our work on XTE J1650−500 (Homan et al. 2003a) we fitted (part of) the resulting power spectra with a sum of Lorentzians, each given by $P(\nu) = (r\Delta/\pi)[\Delta^2 + (\nu - \nu_0)^2]^{-1}$, where ν_0 is the centroid frequency, Δ is the half-width at half-maximum, and r is the integrated fractional rms (from $-\infty$ to ∞). Instead of ν_0 and Δ, we will quote the frequency at which the Lorentzian attains its maximum in $\nu P(\nu)$, $\nu_{\max}$, and the quality factor Q, where $\nu_{\max} = \nu_0(1 + 1/4Q^2)^{1/2}$ and $Q = \nu_0/2\Delta$ (Belloni et al. 2002). The fractional rms amplitudes of the Lorentzians quoted in this paper are the square root of the integrated power between 0 and ∞ (a range that is commonly used). The dead time–modified Poisson noise was approximated by a constant. Errors on fitted parameters were determined using $\Delta\chi^2 = 1$. Upper limits on the strength of the Lorentzians were determined by fixing the Q-value and/or $\nu_{\max}$, but not the rms amplitude, to values similar to those obtained in another power spectrum and using $\Delta\chi^2 = 2.71$ (95% confidence). All quoted significances for QPOs are for single trial. When fitting high-frequency QPOs, we only fitted above ~25 Hz, approximating the noise below 100 Hz with a simple power law. For observations with strong low-frequency QPOs we also performed a study of the phase lags between the 2–5.8 keV (soft) and 5.8–14.9 keV (hard) bands, using methods described in Wijnands et al. (1999).

3. RESULTS

3.1. *Light Curves and Colors*

Figure 1 shows the *RXTE* all-sky monitor light curve (~2–12 keV) of the 2003–2004 outburst of H1743−322 together with X-ray colors (as defined in § 2) from PCA data. The outburst is not of the "classical" fast-rise, exponential-decay type,

[7] For reason of detector preservation, some PCUs were switched off.

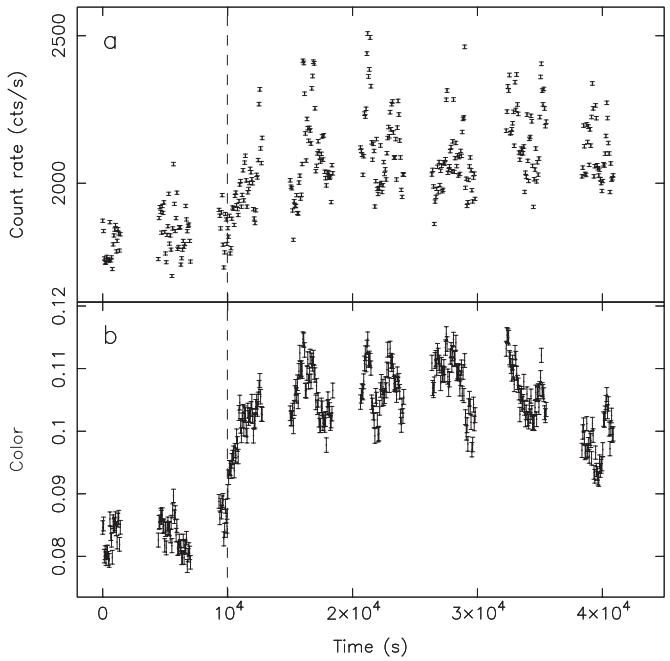

FIG. 3.—Light and color curves of the transition that was seen in observation 2. (*a*) The 2–60 keV light curve. (*b*) Color curve. Both curves are background-subtracted and have time resolutions of 64 s. The dashed line indicates the start of the transition.

showing complex behavior. The dates of our observations are marked by the vertical dotted lines. In Figure 1*b*, which shows the PCA colors, we have also included data from other observations of H1743−322 that were publicly available at the time of writing. The six observations before the vertical dashed line (from program P80138, hereafter observations a–f) were also part of our variability analysis (see § 3.2). These observations clearly show that the source was much harder during the early phase of the outburst than in our observations. Variability studies of the other public observations can be found in Spruit et al. (2004) and Remillard et al. (2004). Average PCA count rates in the 2–60 keV band and the strength of the broadband variability are given in Table 1 for each of our five observations.

The PCA light curves of observations 1–3 showed strong variability with a typical timescale of a few 100 s; an example from observation 1 can be seen in Figure 2. This variability was also observed at lower energies with *Chandra*, but it is stronger at energies above 10 keV, which can be probed by *RXTE* (see Figs. 2 and 5 in Miller et al. 2004). Observation 2 was characterized by a transition in count rate and color that occurred ~10 ks after the start of the observation (see Fig. 3). A sudden jump in color, indicated by the dashed vertical line, occurred within 100 s, but the overall change took about 1000 s. The transition in count rate is less pronounced, but the difference in average count rate before and after is considerable (see Table 1). At the end of the observation the source seemed to become softer again. The light curves of observations 4 and 5 were relatively featureless, showing neither the strong few hundred second variations nor sudden transitions.

3.2. *Low-Frequency QPOs*

In the following we briefly summarize the power spectral properties at frequencies below 100 Hz. The power spectra of our five observations are shown in Figures 4*b*–4*f*. For comparison we have also included a representative power spectrum

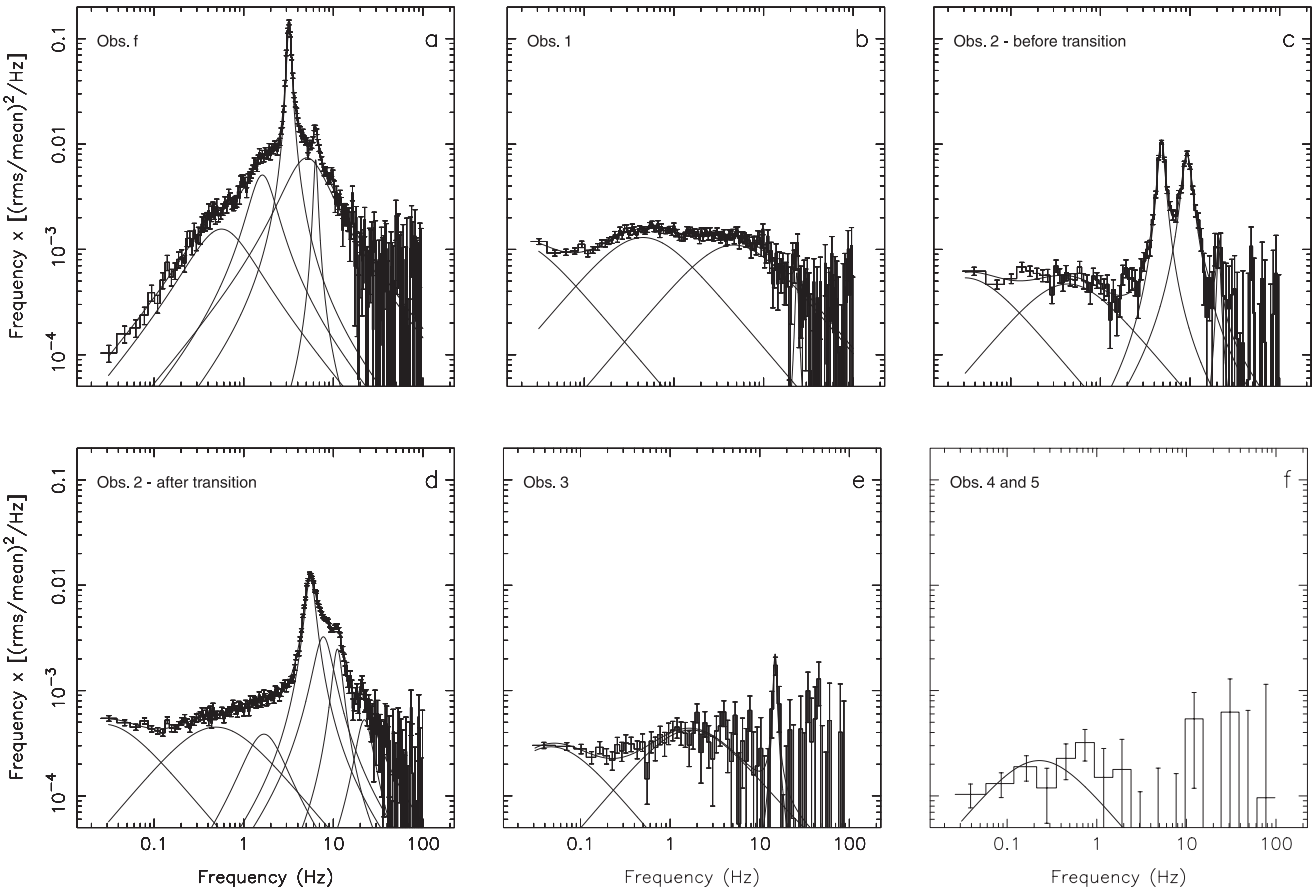

FIG. 4.—Six examples of power spectra observed from H1743−322 in the 5.8–20.9 keV range. For all power spectra the Poisson noise was subtracted. The rebinning was varied between the panels to balance between the frequency resolution and the signal-to-noise ratio. The solid lines indicate the resulting fit function as well as the contribution of the individual Lorentzians.

from the last of the six observations made during the rise (Fig. 4*a*).

Observations a–f.—In all six observations strong band-limited noise was observed, with a QPO around the break. The frequency of this QPO increased from ∼0.06 Hz on March 28 to ∼3.2 Hz on April 10. In Figure 4*a* we show the power spectrum of the April 10 (MJD 52,739) observation as a representative example. The strength of the 0.016–100 Hz variability was $21.4\% \pm 0.1\%$ rms, while that of the QPO at $\nu_{\max} = 3.21 \pm 0.01$ Hz was $15.5\% \pm 0.2\%$ rms. The QPO had a relatively high Q-value of 9.4 ± 0.3. A subharmonic and second harmonic were present at 1.62 ± 0.3 Hz ($Q \sim 1.4$) and 6.37 ± 0.03 Hz ($Q \sim 9.8$). The measured phase lag between the photons in the 5.5–14.9 and 2–5.8 keV bands at the frequency of the 3.2 Hz QPO was 0.0019 ± 0.0009 cycles (of 2π rad), while the phase lags for the sub- and second harmonics were 0.013 ± 0.006 and 0.012 ± 0.003 cycles, respectively. Positive values for the lags indicate that variations in the hard flux are lagging those in the soft band.

Observation 1.—The power spectrum showed red noise with broad structures superposed (see Fig. 4*b*). Three zero-centered (i.e., $Q = 0$) Lorentzians were used to fit the noise continuum. Note that fitting the noise continuum with a broken power law plus a Lorentzian did not result in an improvement. One Lorentzian with $\nu_{\max} = 0.015 \pm 0.007$ Hz fits the red noise component. The other two had $\nu_{\max}$ of 0.45 ± 0.02 and 4.6 ± 0.2 Hz. All three components had fractional rms amplitudes of around 5%. There were hints of a narrow QPO ($Q \sim 10$) around 20 Hz, but it was not significantly detected (∼2 σ). A power spectrum with a lower frequency of $\sim 5 \times 10^{-4}$ Hz revealed a peak in the power spectrum around 0.003 Hz when plotted in a $\nu P(\nu)$ representation (see Fig. 3 in Miller et al. 2004), suggesting a typical timescale of ∼300 s for the variations that are seen in Figure 2.

Observation 2.—Fast changes in variability properties are known to happen in cases of a sudden change in hardness and count rate, such as the one seen in this observation (see Fig. 3). Inspection of the dynamical power spectrum (part of which is shown in Fig. 5) revealed such changes, and we therefore decided to split the observation into two parts, using the time of the sharp transition in color as the divider. The power spectrum of the first part of the observation is shown in Figure 4*c*. It is dominated by red noise and two relatively sharp peaks. The noise was fitted with two zero-centered Lorentzians with $\nu_{\max}$ of 0.033 ± 0.013 and 0.44 ± 0.07 Hz, both with an rms of ∼4%. The two QPOs at $\nu_{\max} = 4.801 \pm 0.014$ and 9.27 ± 0.04 Hz had Q-values of ∼5.3 and ∼3.6, respectively, and strengths of 5%–6% rms. Note that the two peaks appeared not to be exactly harmonically related (ratio $= 1.931 \pm 0.014$), even not when using ν_0 instead of $\nu_{\max}$. Similar cases were reported for QPOs in XTE J1550−564 (Homan et al. 2001; Remillard et al. 2002c), where the nonharmonic ratios were suggested to be caused by evolution of the QPO waveform during the observation or the presence of an additional feature in the power spectrum between the fundamental QPO and its second harmonic. There were no large residuals in the 3−10 Hz

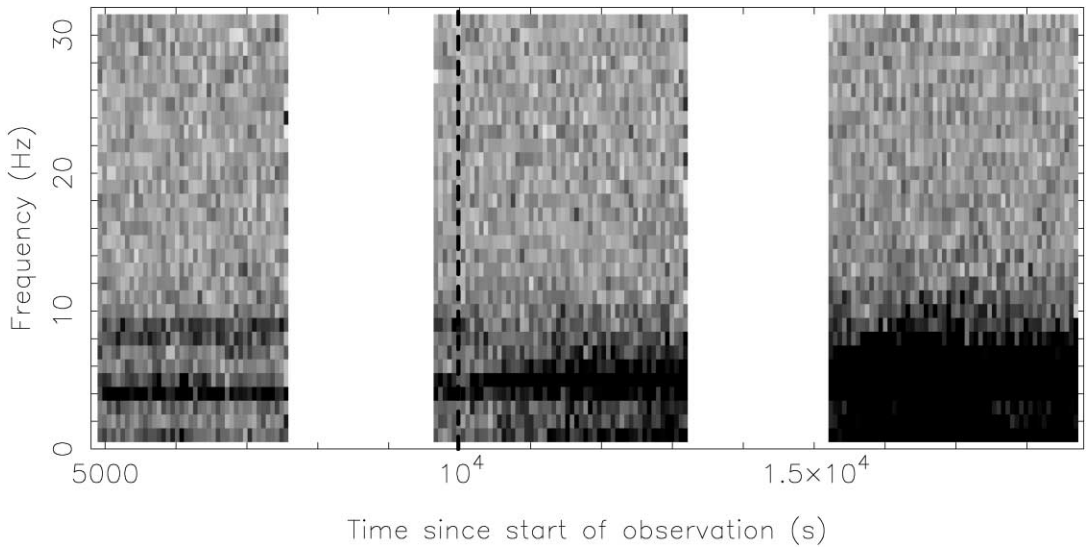

FIG. 5.—Dynamical power spectrum (5.8–20.9 keV) of orbits 2, 3, and 4 of observation 2. Time resolution is 64 s, and frequency resolution is 1 Hz. Darker gray indicates higher power. The two white parts represent gaps in the data. The transition in color that can be seen in Fig. 3*b* occurred around $t = 9980$ s and is indicated in the figure by the dashed vertical line. Note that the harmonic of the type B QPO, which had a frequency of ~9.3 Hz, disappeared shortly after this transition.

range with our fit function that might explain the ratio being different from 2. Nevertheless, we will refer to the second peak as the harmonic in the remainder of the paper. The two peaks had phase lags of -0.069 ± 0.004 and -0.055 ± 0.005 cycles (see also Fig. 6*a*), indicating that the soft photons were lagging the hard photons. Again, we found a hint of a QPO around 20 Hz ($\nu_{\max} \sim 22$ Hz, rms ~ 1.3%, and Q fixed to 10), which in this case was ~3 σ.

The power spectrum of the second part (see Fig. 4*d*) was more complex. Especially the frequency range around the low-frequency QPOs was difficult to fit. The change in the power spectrum between the first and second part (see also Fig. 5) is best described as follows: both the fundamental and its second harmonic increased in frequency by about 15%, to 5.53 ± 0.02 and 11.1 ± 0.1 Hz. The fundamental became less coherent ($Q \sim 3.7$) and increased in strength to ~6.9% rms, while the second harmonic decreased in strength to ~3.3% rms with a similar Q-value. Note that the harmonic was still visible in the dynamical power spectrum, up to the point of the transition. In addition to these changes, a new component appeared at $\nu_{\max} \approx 7.65$ Hz, which had an rms of ~5% and a Q-value of ~1.8. Also, the noise component needed the addition of an extra Lorentzian at $\nu_{\max} \approx 1.7$ Hz ($Q \approx 0.8$ and rms of ~2.4%), while the other two noise components and the QPO at 22 Hz (now detected at a 4.5 σ level, but with a Q of 3.5) remained relatively unchanged. The phase lags of the 5.5 and 11 Hz QPOs were -0.034 ± 0.001 and -0.069 ± 0.002 cycles, respectively. While the sign of the phase lags of the two QPOs remained the same compared to the first part, the overall phase lag spectrum seemed to change, as can be seen from Figure 6*b*. Also, in the case of the QPOs in the second part, no distinct features can be seen in the phase lag spectrum at the frequencies of the QPOs, suggesting that the measured lags are those of the noise continuum. Note that the lags increased above the frequency of the newly detected feature at 7.65 Hz.

Observation 3.—The power spectrum (see Fig. 4*e*) was dominated by red noise, which was fitted with two zero-centered Lorentzians ($\nu_{\max} = 0.046 \pm 0.007$ and $\nu_{\max} = 1.7 \pm 0.2$ Hz), both with a strength of ~1% rms. A narrow ($Q = 11^{+7}_{-3}$) QPO was detected (4.2 σ) at $\nu_{\max} = 14.84 \pm 0.18$ Hz, with an rms of $1.7\% \pm 0.2\%$.

Observations 4 and 5.—The combined power spectrum of these observations (see Fig. 4*f*) was also dominated by red noise. It was fitted with one zero-centered Lorentzian, which had a $\nu_{\max}$ of 0.22 ± 0.08 Hz and an rms of $2.6\% \pm 0.2\%$.

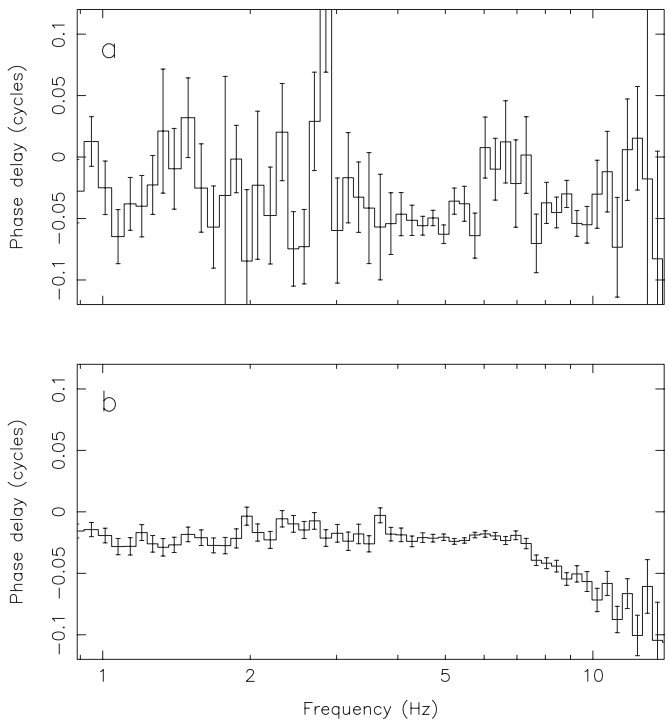

FIG. 6.—Phase lag spectra of the first (*a*) and second (*b*) part of observation 2. The phase lags are in units of cycles of 2π rad and were calculated for the 2–5.8 and 5.8–14.9 keV bands. Negative values indicate that variations in the 2–5.8 keV band lag those in the 5.8–14.9 keV band.

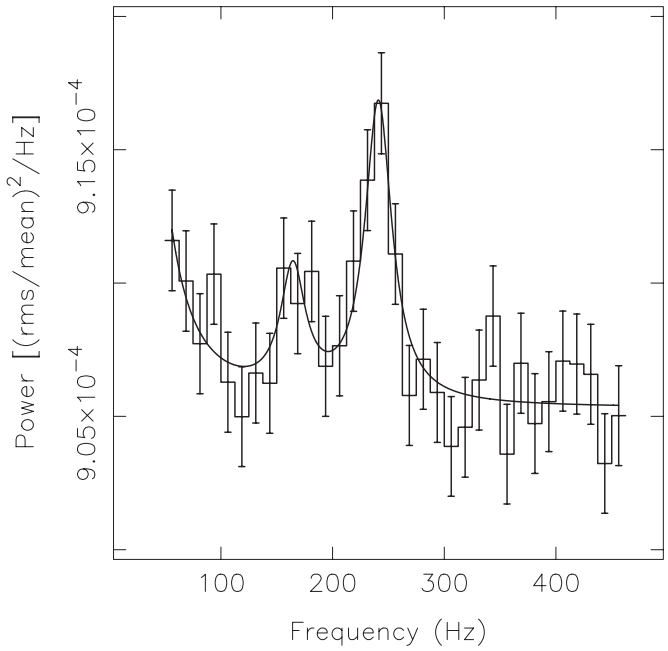

FIG. 7.—High-frequency power spectrum (5.8–20.9 keV) of the second part of observation 2, showing QPOs at 165 and 241 Hz. The Poisson level was not subtracted. The solid line shows the best fits to the power spectrum with a power law and two Lorentzians.

All the above fits had a reduced χ^2 of less than 1.2, except for the fits to the power spectra of observation f and the second part of observation 2, which had a reduced χ^2 of 1.36 and 1.55, respectively. Analysis of other energy bands (3.3–5.8, 5.8–14.9, and 14.9–60 keV) showed that all the QPOs became stronger toward higher energies.

3.3. *High-Frequency QPOs*

All observations were searched for high-frequency QPOs in the 5.8–20.9 keV band. As they are usually only found in observations that show low-frequency QPOs in the 5–10 Hz range, we first searched in observation 2. In that observation a high-frequency QPO was detected at $\nu_{\max} = 240 \pm 3$ Hz. It had an rms of $2.28^{+0.34}_{-0.25}$% (4.5 σ detection) and a Q-value of 7 ± 2. As in the case of the low-frequency part of the power spectrum, we found differences between the first and second part of the observation. In the first part an excess was found at 244^{+26}_{-23} Hz, but only at a 1.8 σ level, with a Q-value of $2.6^{+2.8}_{-1.4}$ and strength of $3.4^{+2.1}_{-0.9}$% rms. A fit to the second part (see Fig. 7) gave $\nu_{\max} = 241 \pm 3$, $Q = 8 \pm 2$, and an rms of $2.20^{+0.28}_{-0.23}$% (4.8 σ detection). Excess power at lower frequencies (~150–180 Hz) was visible in this selection. Fitting this with a second Lorentzian gave a very sharp ($Q \sim 17$) peak at 160 Hz, which only seemed to fit the lower part of the excess. We decided to fix the Q-value to 8 (i.e., the same Q-value as the QPO at 241 Hz), forcing the Lorentzian to fit the whole excess. This gave a frequency of 163^{+5}_{-2} Hz and an rms of 1.29 ± 0.22 (a 3 σ detection). The two measured frequencies had a ratio of 1.47 ± 0.06, consistent with the 3:2 ratio that has been seen in several other black hole X-ray binaries. We also measured the fractional rms amplitudes of the two QPOs in the 3.3–5.8 and 21.0–60 keV bands but only found upper limits: less than 1.2% and 13% for the 163 Hz QPO, and less than 0.6% and 13% for the 241 Hz QPO. Additional selections (only orbits 5–7) revealed an excess below 100 Hz. We added a third Lorentzian to our model, but while the obtained $\nu_{\max}$ of 78 ± 5 Hz ($Q \sim 4$) is suggestive of frequency ratios of 1:2:3, the fit showed that the peak itself was not significant (<2 σ).

None of the other observations showed indications for high-frequency QPOs, but only observation 1 had upper limits on the strength (<1.8% rms) below the values measured in observation 2.

4. DISCUSSION

We studied the variability properties of the black hole transient H1743−322 in five *RXTE* observations that were performed simultaneously with *Chandra* observations, as well as of six observations that were taken at the start of the outburst. The source showed a wide variety of variability properties, including high- and low-frequency QPOs and variability on a timescale of a few hundred seconds. These phenomena are discussed later in this section. First, by comparing the variability properties with the spectral properties of the observations, we attempt to assign X-ray states.

4.1. *X-Ray States*

Observations a–f, at the start of the outburst (before the dashed line in Fig. 1), show a clear spectral evolution. Preliminary spectral fits to the PCU-2 data (see Miller et al. 2004 for a description of data reduction) show that the spectra were dominated by a power-law component with an index increasing from ~1.4 in the first to ~2.4 in the last of the six observations. This, coupled with presence of the strong band-limited noise and QPOs with increasing frequencies of ~0.06–3.2 Hz, suggest that the source was in a transition away from the hard state but had not yet reached the steep power-law state.

The broadband spectral properties of the five *RXTE* observations that were performed (almost) simultaneously with *Chandra* are tabulated in Miller et al. (2004). All spectra were fitted with a combination of a power law and a multicolor disk blackbody. The fractional contribution of the power law to the 3–100 keV flux was about 22% for observations 1 and 3, 50% for the first part of observation 2, ~57% for the second part, and 6% for observations 4 and 5 combined. Observations 4 and 5 are easily classified as soft state (or thermal dominant state), given their low power law flux and low level of variability. Observation 2 is in the steep power law (or very high) state: the power spectrum shows ~6 Hz QPOs on top of moderate red noise, while the energy spectrum shows a steep power law (index of 2.6) that contributes about half of the total flux. We note, however, that although it is sometimes observed in the hard state, strong variability on a timescale of a few hundred seconds is not typical of the steep power law state (Miller et al. 2004 suggest that it may be related to the high source inclination; see below). The same is true for observation 3, which was likely in the soft state. Although the power-law contribution is on the high side for the soft state and the power-law index is quite low (~2.1), the shape and strength of the broadband variability and the presence of a weak QPO around 15 Hz are consistent with the properties of the high-luminosity soft state in XTE J1550−564 (see Homan et al. 2001). Observation 1 is hard to classify. Spectrally it is similar to observation 3, but the broadband noise is stronger (see Table 1 and compare Figs. 4*b* and 4*e*). We note that the higher strength is not due to variations seen in Figure 2, as these occurred on a much longer timescale (i.e., <0.016 Hz). Moreover, similar variability was also seen in observation 3, and from Figure 4 it is clear that flaring is not the dominant source of power below 100 Hz

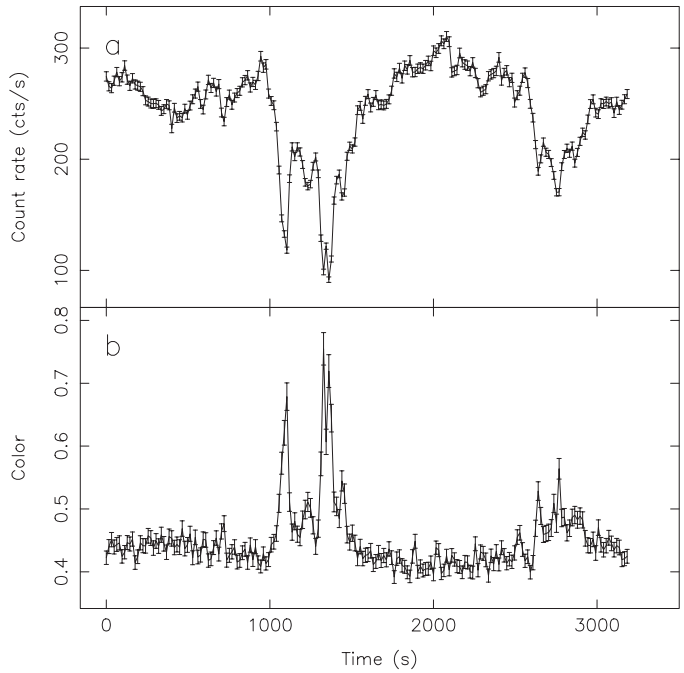

FIG. 8.—(*a*) A 2–5 keV light curve and (*b*) color curve of observation 80146-01-40-00 (MJD 52,776.6) of H1743−322 showing strong dipping on a timescale of tens of seconds. Both curves are from background-subtracted data and have time resolutions of 16 s. For a definition of color, see § 2.

anyway. Based on the spectral and variability properties, we suspect that this observation is intermediate between the steep power law and soft states, although the origin of the broad noise component around 0.5–5 Hz remains unclear.

The above suggests that H1743−322 went through most of the known black hole states. However, we did have some difficulty assigning states to some of our observations. Inspection of data that have become public while this work was in progress revealed strong hard dips in the light curves, with up to 70% decreases at low energies (see Fig. 8). These are similar to dips that have been observed in GRO J1655−40 and 4U 1630−47 (Kuulkers et al. 1998; Tomsick et al. 1998) and suggest a high source inclination ($\sim 60^\circ$–70°). Although a more thorough analysis of those observations is beyond the scope of this paper, a high inclination may explain why some of our observations were difficult to classify.

4.2. *Low-Frequency Variability*

Various types of low-frequency QPOs were observed, which we try to identify with the three types introduced by Wijnands et al. (1999) and Remillard et al. (2002c). Most of the observed QPO properties, such as frequency, *Q*-values, rms, and relation to noise shape/strength, are similar to those observed in other black hole X-ray binaries. Note, however, that the original type A, B, and C definition is solely based on observations of XTE J1550−564, and detailed properties of these QPO types may therefore be different in other sources.

The strong 0.06–3.2 Hz QPOs on top of the band-limited noise in observations a–f were of type C. They showed a large range in frequency and large amplitudes and *Q*-values, and both the fundamental and second harmonic had hard lags. Only the phase lag of the subharmonic had the opposite sign of that observed in XTE J1550−564.

Observations 1–3 showed indications for weak QPOs between 14 and 22 Hz. Such QPOs have so far only been reported for XTE J1550−564 and GRO J1655−40 in their soft states (Homan et al. 2001; Sobczak et al. 2000). It is not clear whether these QPOs are related to any of the three more commonly observed types. Most likely it is not a type A or B QPO, because it was detected simultaneously with QPOs of that type in observation 2 and did not change its frequency when the other low-frequency QPOs did. Fitting the noise continuum in the power spectrum of observation 3 with a broken power law instead of two Lorentzians gives a break frequency of $\sim$5 Hz. Using this frequency and that of the QPO, we find that the source falls on top of the relation between break frequency and QPO frequency that was found by Wijnands & van der Klis (1999) for the black hole X-ray binaries and the Z and atoll type neutron star sources. Note that the points for the soft state QPO in XTE J1550−564 lie close to the relation as well. For that relation Wijnands & van der Klis (1999) only used type C QPOs from black holes, suggesting that the weak 15–22 Hz QPOs in the much softer states might be related to that type. The high *Q*-value of the 15 Hz QPO in observation 3 seems to support such an identification.

Observation 2 showed QPOs around 5–6 Hz, which evolved during (and after) a transition in count rate and color. Before the transition, most of the QPO properties (frequency, strength, and coherence) seem to indicate type B. The only difference is the sign of the phase lag of the fundamental, which was soft, whereas in XTE J1550−564 and XTE J1859+226 it was found to be hard or consistent with zero. After the transition the QPO properties indicate type A (type A-I to be more specific; see Homan et al. 2001). This suggests that for the first time we have observed a smooth transition from a type B to a type A QPO. It also indicates that the two types are more intimately related then previously thought, possibly reducing the number of basic mechanisms for low-frequency QPOs in the 1–10 Hz range to two.

Fast transitions in the light curves of black hole transients (sometimes referred to as "dips" and/or "flip-flops") have been observed in several other systems: GX 339−4 (Miyamoto et al. 1991; Nespoli et al. 2003), GS 1124−68 (Takizawa et al. 1997), 4U 1630−47 (Dieters et al. 2000), XTE J1550−564 (Homan et al. 2001), 4U 1543−47 (Park et al. 2004), and XTE J1859+226 (Casella et al. 2004). In all the cited cases the type of low-frequency variability changed, but because of the shorter transition times, the evolution of the QPO across the transition could not be followed. Casella et al. (2004) found that all of the transitions in XTE J1859+226 involved type B QPOs, which is also true in our case and in the cases reported for XTE J1550−564, GX 339−4 (in the transition reported by Nespoli et al. 2003), 4U 1543−47, and judging from the shape of the QPOs, also in GS 1124−68. In XTE J1859+226 transitions from type B to type A were always found to correspond to increases in the count rate, while transitions from type C to type B correspond to decreases in the count rate. Although an increase in count rate is also observed in our case, the color evolution is opposite to that of the $B \rightarrow A$ transitions in XTE J1859+226 and the overall relation found in XTE J1550−564, suggesting a more complex relation between QPO type and spectral hardness. It is not clear whether differences such as these and different signs of the phase lags of the low-frequency QPOs are related to a higher source inclination.

Three of the observations showed strong variations on a timescale of a few hundred seconds. Although these variations are also seen in the *Chandra* light curves (0.5–10 keV), their relative amplitude becomes about twice as strong toward higher energies (10–25 keV). In observation 2 the $\sim$300 s variability

seemed to be stronger after the transition, which was also seen during a similar transition in GX 339−4 (see Fig. 2 in Nespoli et al. 2003). Miller et al. (2004) found that absorption lines in the *Chandra* spectra were modulated by these variations, which, combined with the suggested high inclination of the source, could imply that the variations might be caused by absorbing or obscuring structures in the observed disk outflow. In that case one would naively expect the modulations to be stronger at lower energies or energy independent, which is the opposite of what we observed. However, variations in the disk outflow itself, which is highly ionized, might lead to stronger variations at higher energies if the wind is able to upscatter photons to higher energies. In observation 3, the 15 Hz QPO is most significantly detected at the lower count rates, which also suggests a more complex relation between these QPOs and the ∼100 s variations than a purely line-of-sight effect. In fact, the latter suggests that the variations might be related to the low-frequency QPOs around 0.01–0.1 Hz, as seen in GRS 1915+105 (Morgan et al. 1997) and 4U 1630−47 (Dieters et al. 2000). In these two sources the 0.01–0.1 Hz QPOs are often simultaneously present with QPOs at higher frequencies (1–10 Hz), whose properties seem to change during the 0.01–0.1 Hz QPO's cycles. However, the dynamical power spectrum of observation 2 (which also showed ∼100 s variations) only shows changes in the QPO frequency related to the transition and not to the few hundred second variations, as in GRS 1915+105 and 4U 1630−47.

4.3. *High-Frequency QPOs*

High-frequency QPOs have recently received considerable attention because of their apparent frequency distribution. In several sources (GRO J1655−40, GRS 1915+105, XTE J1550−564, and possibly XTE J1650−500) evidence has been found for clustering of the high-frequency peaks around frequencies that have ratios that are consistent with 3:2, 3:2:1, or 5:3 (Strohmayer 2001a, 2001b; Miller et al. 2001; Remillard et al. 2002a, 2002b; Homan et al. 2003a). Our detection of simultaneous QPOs at ∼240 and ∼160 Hz in H1743−322 strengthens the idea that a 3:2 ratio is a common feature of high-frequency QPOs in black hole X-ray binaries. We note that the 240 and 160 Hz QPOs have also been detected (at a higher significance) in other observations of H1743−322 by Remillard et al. (2004). In their case the QPOs were found by combining 26 and nine observations, respectively, after selecting on a greater than 7 keV count rate, but they were not detected simultaneously (Remillard et al. 2004). This shows that, as in XTE J1550−564 and GRO J16550−40 (Remillard et al. 2002a), the relative strength of the two harmonically related QPOs in H1743−322 is variable, to the extent that at times only one of them is visible.

Several models have been proposed to explain the frequencies of these high-frequency features, most of them assuming a disk origin of the oscillations (Nowak et al. 1997; Stella et al. 1999; Cui et al. 1998; Psaltis & Norman 2003; Laurent & Titarchuk 2001; Abramowicz & Kluzniak 2003; Rezzolla et al. 2003; Schnittman & Bertschinger 2004). Only in the last three of these references are possible explanations of the observed frequency ratios offered. Abramowicz & Kluzniak (2003) discuss two possible models for the observed 3:2 ratio (they do not discuss the 5:3 ratio observed in GRS 1915+105): the first is the presence of forced 3:1 and 2:1 vertical and radial resonances through pressure coupling (which requires the additional presence of combination frequencies to explain the observed 3:2 ratio), and the second one is parametric resonance between random fluctuations in the (epicyclic) vertical and radial directions. Rezzolla et al. (2003) explain the QPOs as trapped pressure mode oscillations in a torus orbiting a black hole, whose eigenfrequencies are found to be 2:3:4 harmonics. These three resonance models, and in fact most other models, do not explain how the X-ray light curves become modulated at the calculated frequencies. An exception is the model by Schnittman & Bertschinger (2004). These authors used a ray-tracing code in a Kerr metric to explore the light curves of isotropically emitting massive test particles orbiting a rotating black hole. Reasonable amplitudes are retrieved for the simulated modulations, with higher amplitudes being expected for larger viewing angles. The latter seems to be confirmed by the detection of high-frequency QPOs in GRS 1915+105, GRO J1655−40, XTE J1550−564, XTE J1859+226, 4U 1630−47, XTE J1650−500, and H1743−322, all sources that are believed to have moderate to high inclinations (∼50°–75°). Assuming a preference for the particles to occur at or near closed orbits (where ν_r, ν_ϕ, and ν_θ are rational multiples of each other) the authors are able (not surprisingly) to create modulations at a 1:2:3 ratio. More importantly, however, is the elegant way in which they produce changes in the relative strength of these harmonically related peaks (see Remillard et al. 2002a and this work) by varying the arc length of the emission region. In the models of Abramowicz & Kluzniak (2003) and Schnittman & Bertschinger (2004) the QPO frequencies are determined by the spin and mass of the black hole. Estimates of the spin can be made when a mass function of the black hole is available, which is unfortunately not the case yet for H1743−322.

The transition seen in observation 2 provides an opportunity to test the relation between the low- and high-frequency QPOs, since the low-frequency QPOs showed significant changes in their frequency. During the transition the frequency of the low-frequency QPOs increased by ∼15%. Unfortunately, the high-frequency QPO before the transition was not detected at a high significance. However, its frequency (244^{+26}_{-23} Hz) is consistent with the value obtained after the transition (241 ± 3 Hz) and only marginally consistent with 205 Hz (which is 241 Hz: 15%). If the observed constancy of the high-frequency QPO is real, the frequency increase of the low-frequency QPO suggests that the latter is not due to Lense-Thirring precession, as suggested by Schnittman & Bertschinger (2004), since in that case the higher frequency QPO should have changed in frequency as well.

The authors would like to thank the anonymous referee for his/her comments and careful reading of the manuscript. J. H. wishes to thank Ron Remillard and Jeff McClintock for sharing their results prior to publication and Andy Fabian for comments on an early version of the paper. J. H. and W. H. G. L. gratefully acknowledge support from NASA. J. M. M. gratefully acknowledges support from the NSF through its Astronomy and Astrophysics Postdoctoral Fellowship program. T. B. was partially supported by MUIR under CO-FIN grant 2002027145. D. S. acknowledges support from the SAO Clay Fellowship. This research has made use of the data and resources obtained through the HEASARC online service, provided by NASA-GSFC.

REFERENCES

Abramowicz, M. A., & Kluzniak, W. 2003, preprint (astro-ph/0312396)
Baba, D., Nagata, T., Iwata, I., Kato, T., & Yamaoka, H. 2003, IAU Circ., 8112, 2
Belloni, T., Psaltis, D., & van der Klis, M. 2002, ApJ, 572, 392
Bradt, H. V., Rothschild, R. E., & Swank, J. H. 1993, A&AS, 97, 355
Casella, P., Belloni, T., Homan, J., & Stella, L. 2004, A&A, 7707, submitted (astro-ph/0407262)
Cooke, B. A., Levine, A. M., Lang, F. L., Primini, F. A., & Lewin, W. H. G. 1984, ApJ, 285, 258
Cui, W., Zhang, S. N., & Chen, W. 1998, ApJ, 492, L53
Dieters, S. W., et al. 2000, ApJ, 538, 307
Doxsey, R., et al. 1977, IAU Circ., 3113, 2
Emelyanov, A. N., Aleksandrovich, N. L., & Sunyaev, R. A. 2000, Astron. Lett., 26, 297
Fender, R., et al. 1999, ApJ, 519, L165
Grebenev, S. A., Lutovinov, A. A., & Sunyaev, R. A. 2003, Astron. Telegram, 189, 1
Homan, J., et al. 2001, ApJS, 132, 377
———. 2003a, ApJ, 586, 1262
———. 2003b, Astron. Telegram, 162, 1
———. 2004, ApJ, submitted
Jahoda, K., et al. 1996, Proc. SPIE, 2808, 59
Jain, R. K., Bailyn, C. D., Orosz, J. A., McClintock, J. E., & Remillard, R. A. 2001, ApJ, 554, L181
Kalemci, E., Tomsick, J. A., Rothschild, R. E., Pottschmidt, K., & Kaaret, P. 2004, in AIP Conf. Proc. 714, X-Ray Timing 2003: *Rossi* and Beyond, ed. P. Kaaret, F. K. Lamb, & J. H. Swank (Melville: AIP), 52
Kaluzienski, L. J., & Holt, S. S. 1977a, IAU Circ., 3099, 3
———. 1977b, IAU Circ., 3106, 4
Kretschmar, P., et al. 2003, Astron. Telegram, 180, 1
Kuulkers, E., et al. 1998, ApJ, 494, 753
Laurent, P., & Titarchuk, L. 2001, ApJ, 562, L67
Markwardt, C. B., & Swank, J. H. 2003a, Astron. Telegram, 133, 1
———. 2003b, Astron. Telegram, 136, 1
McClintock, J. E., & Remillard, R. A. 2004, in Compact Stellar X-Ray Sources, ed. W. H. G. Lewin & M. van der Klis (Cambridge: Cambridge Univ. Press), in press (astro-ph/0306213)
Miller, J. M., et al. 2004, ApJ, submitted (astro-ph/0406272)
———. 2001, ApJ, 563, 928
Miyamoto, S., Kimura, K., Kitamoto, S., Dotani, T., & Ebisawa, K. 1991, ApJ, 383, 784
Morgan, E. H., Remillard, R. A., & Greiner, J. 1997, ApJ, 482, 993
Muno, M. P., Morgan, E. H., & Remillard, R. A. 1999, ApJ, 527, 321
Nespoli, E., et al. 2003, A&A, 412, 235
Nowak, M. A., Wagoner, R. V., Begelman, M. C., & Lehr, D. E. 1997, ApJ, 477, L91
Park, S. Q., et al. 2004, ApJ, 610, 378
Parmar, A. N., et al. 2003, A&A, 411, L421
Psaltis, D., & Norman, C. 2003, ApJ, submitted
Remillard, R. A., McClintock, J. E., Orosz, J. A., & Levine, A. M. 2004, ApJ, submitted (astro-ph/0407025)
Remillard, R. A., Muno, M. P., McClintock, J. E., & Orosz, J. A. 2002a, ApJ, 580, 1030
———. 2002b, in New Views on Microquasars: the Fourth Microquasars Workshop, ed. Ph. Durouchoux, Y. Fuchs, & J. Rodriguez (Kolkata: Center for Space Physics), 49
Remillard, R. A., Sobczak, G. J., Muno, M. P., & McClintock, J. E. 2002c, ApJ, 564, 962
Revnivtsev, M., et al. 2003, Astron. Telegram, 132, 1
Reynolds, A. P., et al. 1999, A&AS, 134, 287
Rezzolla, L., Yoshida, S., Maccarone, T. J., & Zanotti, O. 2003, MNRAS, 344, L37
Rupen, M. P., Mioduszewski, A. J., & Dhawan, V. 2003, IAU Circ., 8105, 3
Schnittman, J. D., & Bertschinger, E. 2004, ApJ, 606, 1098
Sobczak, G. J., et al. 2000, ApJ, 531, 537
Spruit, H. C., Steinle, H., & Kanbach, G. 2004, preprint (astro-ph/0404524)
Steeghs, D., Miller, J. M., Kaplan, D., & Rupen, M. 2003, Astron. Telegram, 146, 1
Stella, L., Vietri, M., & Morsink, S. M. 1999, ApJ, 524, L63
Strohmayer, T. E. 2001a, ApJ, 552, L49
———. 2001b, ApJ, 554, L169
Takizawa, M., et al. 1997, ApJ, 489, 272
Tanaka, Y., & Lewin, W. H. G. 1995, in X-Ray Binaries, ed. W. H. G. Lewin, J. van Paradijs, & E. P. J. van den Heuvel (Cambridge: Cambridge Univ. Press), 126
Tomsick, J. A., & Kalemci, E. 2003, Astron. Telegram, 198, 1
Tomsick, J. A., Lapshov, I., & Kaaret, P. 1998, ApJ, 494, 747
van der Klis, M. 1995a, in X-Ray Binaries, ed. W. H. G. Lewin, J. van Paradijs, & E. P. J. van den Heuvel (Cambridge: Cambridge Univ. Press), 252
———. 1995b, in NATO ASI Ser. 450, The Lives of the Neutron Stars, ed. M. A. Alpar, U. Kiziloglu, & J. van Paradijs (Dordrecht: Kluwer), 301
White, N. E., & Marshall, F. E. 1983, IAU Circ., 3806, 2
Wijnands, R., Homan, J., & van der Klis, M. 1999, ApJ, 526, L33
Wijnands, R., & van der Klis, M. 1999, ApJ, 514, 939
Wood, K., Share, G., Johnson, N., Yentis, D., & Byram, E. T. 1978, IAU Circ., 3203, 1